Effects of Canopy Structural Variables on Retrieval of Leaf Dry Matter Content and Specific Leaf Area From Remotely Sensed Data

Abebe Mohammed Ali, Roshanak Darvishzadeh, Andrew K. Skidmore, and Iris van Duren

***Abstract*—Leaf dry matter content (LDMC) and specific leaf area (SLA) are two important traits in measuring biodiversity. To use remote sensing for the estimation of these traits, it is essential to understand the underlying factors that influence their relationships with canopy reflectance. The effect of canopy structures—particularly stem density (SD), leaf area index (LAI), stand height (SH), crown diameter (CD), and average leaf angle (ALA)—on the relationship between LDMC and SLA with the canopy reflectance were investigated using a canopy reflectance dataset simulated by the invertible forest reflectance model (INFORM) radiative transfer model. The parameterization of the model was based on the range of the field parameters collected in the Bavarian National Park in July 2013 and the configuration of the HYSpex hyperspectral sensor. Strong correlations were observed between the two leaf traits and indices derived from simulated canopy spectra in the NIR and SWIR region ($\mathbf{R^2}$ values of 0.87 for LDMC and 0.85 for SLA). Among the tested HYSpex wavelengths, the bands most sensitive to variation were 2298.69 nm for LDMC and 2280.71 nm for SLA. The effects of the stated structural variables on the relationships were best controlled by the modified normalized difference (mND) vegetation index (VI): ($[\mathbf{R2275 - R1920}]/[\mathbf{R2275 + R1920 - 2 * R1520}]$). The structural variables that most affected the relationship were forest SD and CD. The modeling results suggest that the spectral variation due to changes in LDMC and SLA is best captured for stands with $\mathbf{SD > 400\ trees/ha}$ and $\mathbf{CD \geq 5\ m}$. The influence of LAI and SH on the relationships can be greatly reduced using VIs. We conclude that LDMC and SLA can be accurately estimated from canopy reflectance, irrespective of the heterogeneity of structural variables, providing that canopy cover exceeds 50%.**

***Index Terms*—Canopy structural variables, invertible forest reflectance model (INFORM), leaf dry matter content (LDMC), leaf traits, radiative transfer, specific leaf area (SLA).**

I. Introduction

LEAF DRY matter content (LDMC) and specific leaf area (SLA) are two fundamental functional traits in biodiversity. LDMC is the ratio of the dry mass of a leaf to its fresh mass expressed in mg/g. It reflects plant growth rate [1], carbon assimilation, and resource usage and availability [2], whereas SLA is the ratio of leaf area to leaf dry mass, usually expressed in cm^2/g [3]. SLA links plant carbon and water cycles, and provides information on the spatial variation in photosynthetic capacity and leaf nitrogen content (e.g., 4, 5, and 6). SLA is also indicative of plant physiological processes such as light capture, growth rates, and life strategies of plants [4]. Leaf traits are generally correlated with each other [7]–[9]. As a result, LDMC and SLA are interdependent, and have been used to estimate (or predict other ecological indicators, such as leaf thickness [10]–[12], relative growth rate [13], and soil fertility [14]. They are increasingly used to investigate community structure and ecosystem functioning [15]–[19]. Since the focus of biodiversity research is shifting from species diversity to functional diversity [20], accurately measuring these traits is therefore of prime importance.

Plant functional traits can be retrieved from remotely sensed data using either statistical (inductive) approaches or physically based models (deductive approaches) [21]. The statistical approaches investigate the relationship between vegetation variables and their spectral reflectance or some derivative of reflectance. Vegetation indices (VIs) are the most common statistical methods utilized, due to their simplicity. An alternative is to use radiative transfer models (RTM) or so-called physical models, which mimic the transfer and interaction of solar radiation inside the canopy and simulate the reflectance of a given canopy (specific situation). They offer an explicit connection between the vegetation variables and traits and the canopy reflectance [22]. Although remote sensing is a fast and cost-effective alternative, acquiring information on functional traits is still mainly restricted to field observation, which is labor-intensive and time-consuming. In particular, hyperspectral remote sensing (often called imaging spectroscopy) has the advantage of providing detailed and continuous spectral information which can be potentially used for measuring plant functional traits (e.g., [23], [24]–[27]).

Over the last four decades, several statistical methods and RTMs have been developed to estimate biochemical and biophysical variables at leaf and canopy levels, using hyperspectral data (e.g., [28], [29]–[31]). Both approaches have been applied to estimate vegetation biophysical and biochemical variables from remotely sensed data (e.g., [32]–[34]) and they have also been compared in terms of their efficacy in estimating vegetation variables in grasslands from hyperspectral imagery [35].

However, when the observational scale moves from leaf to canopy scale, the relationship between reflected radiation and

Manuscript received January 01, 2015; revised June 05, 2015; accepted June 21, 2015. Date of publication July 22, 2015; date of current version February 09, 2016. The work of A. M. Ali was supported by the Nuffic Netherlands Fellowship Program (Nuffic-nfp).

The authors are with the Faculty of Geo-Information Science and Earth Observation (ITC), University of Twente, 7500 AE Enschede, The Netherlands (e-mail: a.m.ali@utwente.nl; r.darvish@utwente.nl; skidmore@itc.nl; vanduren@itc.nl).

Color versions of one or more of the figures in this paper are available online at http://ieeexplore.ieee.org.

Digital Object Identifier 10.1109/JSTARS.2015.2450762

leaf traits tends to weaken [36]. The scattering and absorption properties caused by leaf traits are then confounded by soil, nonphotosynthetic vegetation (litter, bark, and branches), stem characteristics, canopy structure, and shadows [37]–[39]. Indices that have originally been designed at leaf scale are particularly likely to suffer from these additional heterogeneity factors when used at canopy (i.e., larger) scale [36], [38], [40]. Therefore, understanding the impact of these factors on canopy reflectance is a crucial first step toward accurately estimating the desired vegetation variables using remote-sensing approaches. Sensitivity analysis enables the investigation of the influence of the targeted variable and the confounding factors on canopy reflectance. This, in turn, gives information on the potential to successfully retrieve variables by using statistical or RTM inversion methods from remotely sensed data [41].

Several studies have attempted to examine the sensitivity of RTMs and VIs in quantifying biochemical variables. The effect of soil types and soil properties on canopy reflectance is well documented in the literature [42]–[46]. Asner [47] revealed LAI and leaf angle distribution as the dominant determinants of canopy reflectance if canopy closure (CC) and soil effect are controlled. A study by Barton and North [48] has concluded that the positive correlation between photochemical reflectance index and photosynthetic light use efficiency is influenced by solar zenith, leaf area index (LAI), leaf angle distributions, and soil types when using photochemical models. Bowyer *et al.* [49] compared the performance of local and global sensitivity analysis methods in determining the sensitivity of reflectance data to the input parameters of the PROSPECT and GeoSAIL RTMs. Bannari *et al.* [50] analyzed the sensitivity of Chlorophyll Indices to Soil Optical Properties and demonstrated that chlorophyll indices are less sensitive to changes in soil optical properties and can be used for a better estimation of chlorophyll content in a sparse crop cover environment. The influences of nonphotosynthetic vegetation and CC on chlorophyll [51] and LAI retrieval [52] have also been investigated for various canopy situations using single bands and VIs on an RTM-simulated dataset. A recent study by Xiao *et al.* [53] using Prospect_5 and 4SAIL RTM at different levels reported the sensitivity of reflectance to the variation in vegetation variables such as leaf chlorophyll content, leaf mass area, leaf water content, LAI, and vegetation fractional cover. Review of the literature revealed that there have not been many studies involving stem density (SD) and stand height (SH). Therefore, more studies need to be conducted to examine the effect of these structural variables on canopy reflectance.

Although LDMC and SLA are keystone ecological parameters, the efforts made to estimate these parameters from remotely sensed data are rare. It is only recently that a study at leaf scale using the PROSPECT model has shown that LDMC and SLA can be accurately estimated from remotely sensed data and has recommended upscaling and extension of the inversion to the canopy scale [54]. To our knowledge, no study has examined the impact of canopy structural variables on the estimation accuracy of LDMC and SLA from remotely sensed data. Therefore, here, we investigated the influence of key canopy structural variables such as single-tree LAI (LAI_s), SD, SH, crown diameter (CD), and average leaf angle (ALA) on LDMC and SLA retrieval using an RTM. Specifically, three aims were addressed. 1) It was examined whether there is a significant canopy reflectance variation due to changes in LDMC and SLA content. 2) The performance of selected wavelengths and several VIs in retrieving LDMC and SLA under various canopy situations was evaluated. 3) The stand-specific impact of LAI_s, SD, and SH on the estimation of LDMC and SLA was assessed in detail.

II. Methodology

A. Test Site and Field Data

The sensitivity of canopy reflectance to the desired plant functional traits and confounding structural variables was analyzed based on RTM simulation of the mixed mountain forest of the Bavarian Forest National Park. The park is located in southeastern Germany along the border with the Czech Republic ($49^\circ\ 3'\ 19''$ N, $13^\circ\ 12'\ 9''$ E). Elevation varies from 600 to 1473 m above sea level. The climate of the region is temperate, with high annual precipitation (1200–1800 mm) and low average annual temperature (3 °C–6 °C). Heavy snow cover is characteristic of the area in winter. Spodosols are the predominant soil type at lower altitude (below 900 m asl), whereas at high altitude (above 900 m asl), spodosols and brown podzolic soil predominate. The soils in the area are naturally acidic and low in nutrient content [55]. The natural forest ecosystems of the Bavarian Forest National Park vary with altitude: there are alluvial spruce forests in the valleys, mixed mountain forests on the hillsides, and mountain spruce forests in the high areas. The dominant tree species include European beech (*Fagus sylvatica*), Norway spruce (*Picea abies*), and Fir (*Abies alba*). In the mixed mountain forests, Sycamore maple (*Acer pseudoplatanus L*), Mountain ash (*Sorbus aucuparia L*), and Goat willow (*Salix caprea*) are also found [56].

A field campaign was conducted between July 11 and August 23, 2013. The study area was stratified into broadleaf, conifer, and mixed forest stands. Considering the nature of the forest heterogeneity, time, and cost constraints, 26 plots (8 broadleaf, 6 conifer, and 12 mixed stands) were randomly selected within each forest stand. Each plot was square, with sides 30 m long. At each plot, leaf samples were collected and structural variables were measured. The collected leaf samples were transported to a laboratory. For every sample, LDMC, SLA, leaf mass per area (C_m), and leaf water content (C_w) were computed from samples fresh and oven-dried mass at 65 °C for 48 h. The leaf samples' hemispherical reflectance and transmittance from 350 to 2500 nm with 1-nm spectral resolution were also measured using a FieldSpec3 portable spectroradiometer equipped with an integrating sphere manufactured by Analytical Spectral Devices, Inc. (ASD), USA; see [54] for details of the leaf samples' physical variables and spectral measurements. The measured forest structural variables were LAI, SD, CC, CD, SH, and ALA. LAI and ALA were computed from hemispherical photographs taken in each plot by using CIMES-FISHEYE software [57]. SD was recorded as number of trees per hectare, based on the number of trees in each plot. CC was estimated by averaging five observations in a plot, using a crown densiometer. CD and SH were calculated from

TABLE I
SUMMARY STATISTICS OF THE MEASURED LEAF ($n = 137$) AND CANOPY STRUCTURAL VARIABLES ($n = 26$) IN BAVARIAN FOREST, LEAF MASS PER AREA (C_m), LEAF WATER CONTENT (C_w), LEAF DRY MATTER CONTENT (LDMC), SPECIFIC LEAF AREA (SLA), LEAF AREA INDEX (LAI), STEM DENSITY (SD), CANOPY CLOSURE (CC), CROWN DIAMETER (CD), AND STAND HEIGHT (SH)

Basic statistics	N=137				N=26					
Parameter	C_m (g/cm^2)	C_w (g/cm^2)	LDMC (mg/g)	SLA (cm^2/g)	LAI	SD (n/ha)	CC (%)	CD (m)	SH (m)	ALA (degree)
Minimum	0.0034	0.0063	337.3	34.36	2.79	222	77	1.65	8	38
Maximum	0.0291	0.0337	598.4	294.09	6.21	1722	91	15.45	38	50
Mean	0.0140	0.017	455.2	93.45	4.6	771	81.5	5.4	23	61
Standard deviation	0.0030	0.0032	42.95	24.58	0.72	461	4.6	2.2	4.6	9.9

mean CD and mean height of five trees randomly selected in each plot. The CD of each tree was determined by averaging two perpendicular projected distances on the ground. The total height of each tree was estimated by using a Nikon Forestry 550 laser rangefinder. The measured physical and structural variables from the field are summarized in Table I. During the field campaign, the spectral reflectance characteristics of understory vegetation and ecosystem elements in the forest floor such as bark, litter, mosses, and lichens were also measured by using the ASD field spectroradiometer coupled to a high intensity contact probe.

B. Canopy RTM Selection

A large variety of canopy RTMs is currently available and a recent comparison is presented by Widlowski *et al.* [58]. There are four broad categories of canopy reflectance models: 1) the one-dimensional (1-D) or turbid media models (e.g., the SAIL [59]); 2) geometric optical models (e.g., GOST [60]; 3) Monte Carlo ray tracing three-dimensional (3-D) models (e.g., DART model [61]), which stochastically calculate photon trajectories within turbid or geometric canopies; and 4) hybrid models (e.g., GEOSAIL [62]), which combine elements of the turbid medium, the geometric optical, and the ray tracing models.

The canopy RTM should be adjustable to canopy compositional variability. It is crucial to select a model that is capable of accurately representing the complex forest structure with minimal input requirements to build scenes of a forest canopy. Simple turbid medium (1-D) RTMs are unlikely to be able to account for changes in structural composition. Geometric optical models simulate bidirectional reflectance as a purely geometric phenomenon by considering the shape of objects, their count densities, and patterns of placement as driving variables, but do not count the interaction between elements due to multiple scattering among leaves and individual canopies [63]. Ray-tracing models and hybrid models that have 3-D functionalities are expected to be better equipped to simulate the radiative transfer fluxes within a heterogeneous canopy, but often the amount of a priori knowledge needed to build the description of a canopy can be a limiting factor. Among the hybrid models, the invertible forest reflectance model (INFORM) [28], [64] seems to be particularly suitable with respect to linking canopy variables to reflectance data while preserving simplicity in generating scenes.

INFORM is a combination of the forest light interaction model [65] and SAIL [59] canopy RTMs with the PROSPECT [29] leaf RTM. INFORM is parameterized by leaf parameters, such as C_m, C_w, and chlorophyll content; canopy parameters, such as SD, LAI_s, and SH; and external parameters, such as sun zenith (θ_s) and sun azimuth angle (Ψ), and simulates canopy spectral reflectance of forest stands between the 400- and 2500-nm wavelengths. Unlike the 3-D RTMs, the outputs of INFORM are not simulated images. It provides spectral signatures on top of a canopy under well-specified conditions. In other words, the simulated spectra are independent of spatial resolution. The influence of the structural variables on LDMC and SLA retrieval was investigated on simulated data using the coupled leaf and canopy RTM-INFORM. All possible canopy structural compositions of LAI_s, SD, SH, CD, and ALA that may occur in the test site were considered during the simulation.

C. INFORM Parameterization and Forest Reflectance Simulation

The structural variables (SD, LAI_s, SH, CD, and ALA) addressed in this study were among the main structural components that greatly vary throughout the forest stands in the Bavarian Forest National Park. To study the effect of the confounding factors, a relationship should be established between the confounding variables with LDMC and SLA (hereafter referred to as “the two leaf traits”) for any given canopy structure or composition that could occur in the test site. Thus, INFORM was parameterized on the basis of Bavarian National Park Forest leaf and stand characteristics. The model input parameters, C_m, C_w, LAI_s, SD, SH, CD, ALA, θ_s, and Ψ were generated using a uniform distribution based on the available range of the ground-truth data (Table I).

Other leaf, canopy, and external input parameters were fixed to average values based on the ground-truth data, sensor (HYSpex) specification, and previous studies [54]. In INFORM, LAI is represented by LAI_s. Hence, the range for LAI_s was estimated by computing LAI_s from LAI and CC as $LAI_s = LAI/CC$. For every combination of input parameters, LDMC and SLA were indirectly calculated from C_m and C_w as $LDMC = C_m/(C_m + C_w)$ and $SLA = 1/C_m$ (see [54] for details). The input parameter values used for forest canopy reflectance simulation with INFORM are presented in Table II.

The simulation was done without the presence of atmosphere on top of the canopy. Bare soil occurred extremely rarely on the forest floor. Hence, the field spectra of understorey vegetation and the forest floor elements were averaged and used as a fixed background reflectance during the simulation.

TABLE II
INPUT PARAMETERS USED DURING INFORM SIMULATION BASED ON FIELD OBSERVATION AND PREVIOUS STUDIES

Input variable	Symbol	Unit	Mean	Range of simulated variation		
				Min	Max	Step
Leaf dry mass per area	C_m	g/cm^2	0.014	0.0034	0.0291	0.005
Equivalent water thickness	C_w	g/cm^2	0.017	0.0063	0.0337	0.005
Leaf structural parameter*	N	NA	1.5			
Chlorophyll content*	C_{ab}	g/cm^2	40			
Single tree LAI	LAI_s	NA	4.0	2	8	0.5
Understorey LAI	LAI_u	NA	0.1			
Stem density	SD	n/hr	771	200	1800	150
Stand height	SH	M	23	8	38	5
Crown diameter	CD	M	5.4	3	11	2
Average leaf angle	ALA	Degree	50	40	60	5
Sun zenith angle	θ_s	Degree	32	20	80	20
Observation zenith angle	θ_0	Degree	0			
Azimuth angle	Ψ	Degree	153	100	200	30
Fraction of diffused radiation*	Sky1	Fraction	0.1			

*Fixed based on previous studies.

The shortwave-infrared region is reported as the most sensitive region for retrieving parameters related to dry matter [23], [66]–[68]. This region also avoids the need to measure leaf pigments for model calibration and validation, since they have no impact on the selected range spectral signature [66]. Therefore, the forest canopy spectral reflectance was simulated in 309 spectral wavelengths (800–2500 nm) corresponding to the near-infrared (NIR) and shortwave-infrared (SWIR) band settings of the HYSpex system developed by the Norwegian company Norsk Elektro Optikk. The HYSpex system comprises two imaging spectrometers with spectral ranges of 400–1000 and 1000–2500 nm and up to 416 spectral channels at high spatial resolution. The HYSpex system records radiance data in contiguous bands at a spectral resolution of 3.7 nm for 400–992 nm spectral range (sensor 1) and 6 nm for 968–2498 nm spectral range (sensor 2). It has a spatial resolution of 1.6 m for sensor 1 and 3.3 m for sensor 2. The HYSpex instrument was flown over the study site on board a Cessna 208B Grand Caravan at average altitudes of 3006.5 m above sea level on July 22, 2013 between 9:00 and 11:15 local time. The German earth observation center has successfully tested the system and made it available to the remote-sensing community [69]. The solar zenith and azimuth angles were set close to the range of the Bavarian National Park overflight settings and the view zenith angle was set at nadir.

D. Confounding Factors Affecting LDMC and SLA Retrieval

Using the INFORM model, a total of 8 108 100 forest canopy spectra ($6\ C_m \times 6\ C_w \times 13\ LAI_s \times 11$ SD $\times$ 7 SH $\times$ 5 CD $\times$ 5 ALA $\times$ 4 θ_s $\times$ 3 Ψ) were simulated and used for the subsequent analysis of the contribution of each targeted variable to the spectral signal at stand scale. The analysis attempted to evaluate the suitability of imaging spectroscopic-based approaches for estimating LDMC and SLA. Several VIs based on a previous study by le Maire *et al.* [70], who evaluated the performance of different types of VIs for leaf mass per area retrieval in a forest canopy, were used and assumed to be sensitive to LDMC and SLA. These indices and their individual wavelengths were adjusted to the HYSpex band configurations (Table III).

TABLE III
VEGETATION INDICES USED FOR THE SENSITIVITY ANALYSIS OF LDMC AND SLA AGAINST THE CONFOUNDING FACTORS (LAI_S, SD, AND SH)

Index type	Original formula	Formula in HYSpex bands
Difference (D)	R2380−R2300	R2382.63−R2298.69
Simple ration (SR)	R2280/R1395	R2280.71/R1393.44
Normalized difference (ND)	(R2280−R1395)/ (R2280+R1395)	(R2280.71−R1393.44)/ (R 2280.71+R1393.44)
Modified normalized Difference (mND)	(R2275−R1920)/ (R2275+R1920−2*R1520)	(R2274.71−R1921.01)/ (R2274.71+R1921.01−2*R1519.34)
Modified simple ratio (mSR)	(R2275−R1921.01)/ (R1920−R1520)	(R2274.71−R1921.01)/ (R1921.01−R1519.34)
Normalized difference (ND)	(R2260−R1490)/ (R2260+R1490)	(R2262.72−R1489.36)/ (R2262.72+R1489.36)

The indices are those studied in le Maire *et al.* [70].
NB: All the HYSpex bands involved in the indices calculation were also individually tested for their sensitivity to the two leaf traits and confounding factors analysis.

The effects of confounding factors on LDMC and SLA were analyzed by studying how the variations in the confounding factors change the relationship between the two leaf traits and the spectral bands or spectral indices. To test which of the input parameters (the two leaf traits, LAI_s, SD, SH, CD, or ALA) determines most of the spectral variation in the forest canopy spectra simulations at various sun zenith and azimuth angles, we used analysis of variance (ANOVA) to decompose the total variance into terms related to the individual factors. First, the sensitivity of the simulated spectra for the variation in the two leaf traits and different combinations of the confounding factors was tested for its statistical significance, using an F-test. ANOVA computes the variance as the sum of squared deviations. In our case, the sum of squares of the simulations was partitioned into a sum of squares related to the overall mean, a sum of squares related to the treatment effects, and a residual sum of squares.

To test whether a specific band (or index) is sensitive to the two leaf traits, the F-statistic for LDMC and SLA was used. To test the sensitivity for the two leaf traits relative to the factors (LAI_s, SD, SH, CD, and ALA), an F-statistic was calculated by dividing the mean square related to the two leaf traits by the mean square related to each of the factors. The best spectral band (index) for LDMC and/or SLA estimation is the one that has the largest calculated F-value. Pairwise multiple comparison tests were then done for the spectral bands and spectral indices with a significant F-test result, using the least significant difference (LSD), which is the widely used post hoc analysis, to determine which values of a given factor differ significantly from each other. Coefficients of determination (R^2) between the two traits and each of the selected spectral bands (index) were also computed and used for evaluating the correlation strength of the HYSpex canopy reflectance (indices) to the two leaf traits.

Second, the LDMC and SLA effects on the spectral band or spectral index with high significance value were further analyzed for each combination of confounding variables. The two traits' variations were plotted against the best-performing bands and indices in the F-test, and the effect of each selected structural variable was examined individually, keeping all other variables constant. The relationship between the two leaf traits' variation and the reflectance was measured by means of local sensitivity analysis.

We chose the local sensitivity analysis method because the model simulation was run by varying the two leaf traits and the five confounding variables at variable solar zenith and azimuth angles, keeping all other parameters constant as shown in Table II. In the other sensitivity analysis method (global sensitivity analysis), all the input parameters vary simultaneously [49]. From the results yielded by local and global sensitivity analyses, it appears that these analyses alter the magnitude of the importance of the factors under investigation [49]. Slopes of relationships between the leaf traits and the structural variables were used to measure the sensitivity of the selected index for variation in the two leaf traits. The derivative (∂y/∂x) was computed from the relationship between the two leaf traits' content (x variable) and VI (y variable) for every combination of the two leaf traits' intervals and confounding variables from the INFORM-generated reflectance spectra. The average slope was then calculated as the derivative averaged over all intervals for a stand-specific situation. The steeper the slope, the more accurate is the estimation of the two leaf traits. Thus, the average slope was considered as a stand-specific indicator of the two leaf traits' detectability.

Third, the combined effects of the confounding factors on the two leaf traits were investigated by pairing up two factors at a time, while other variables were kept constant at the observed average value in the test site. For instance, the combined effect of LAI_s and SD was evaluated by keeping SH, CD, and ALA values at their averages in the test site. For simplicity, the steps were only repeated for possible combinations of LAIs, SD, and H confounding factors. Plotting the average slopes for each of these paired combinations provided three scenarios of canopies that might occur in heterogeneous forest. The sensitivity analysis was finalized by establishing a link between the modeling results and structural information measured in the Bavarian National Park mixed mountain forest canopies.

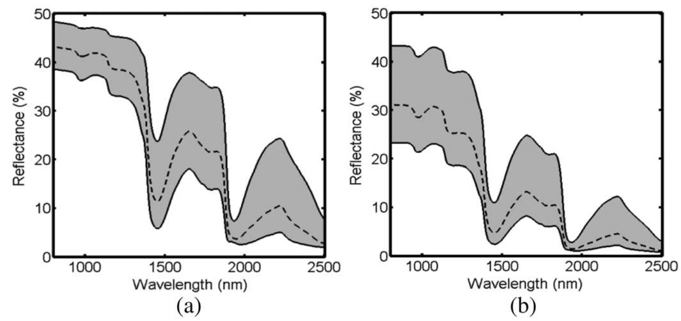

Fig. 1. Simulated reflectance at (a) leaf scale and (b) canopy scale as simulated by INFORM using the input parameters presented in Table II. The dashed lines show the mean and the shaded areas show the ranges of the simulated reflectance.

III. Results

A. Spectral Variation Due to LDMC and SLA

Before testing the strength of spectral variation caused by the two leaf traits, we checked the trend of reflectance variation when the scale moves from leaf to canopy level. Fig. 1 shows how the mean and standard deviation (std) of the simulated reflectance shifts with upscaling. Upscaling from leaf to canopy level increased the spectral variation in the NIR region and diminished the spectral variation in the SWIR region. The overall spectral variation at canopy level (std of 12.14%) is lower than the leaf scale (std of 15.39%). Nonetheless, strong correlations between the two traits and canopy reflectance (indices) were observed (see Tables IV and V).

The canopy scale reflectance was further evaluated using the F-test to ascertain whether the spectral variation due to LDMC and SLA in the presence of canopy confounding factors is significant. The results from single-band tests are summarized in Table IV. The larger the F-test value, the more assurance that the band is more sensitive to LDMC and/or SLA than the other factors, meaning that the impact of the structural variables variation is much less than that of LDMC and/or SLA variation. Among the selected HYSpex wavelengths, the band at 2298.69 nm was the most sensitive band for variation in both LDMC and SLA. The band at 2280.71 nm also showed strong correlation to variation in SLA. The selected bands showed stronger correlation with LDMC than SLA. A substantial amount of influence on spectral variation originated from the structural variables SD, CD, and ALA and the least disturbing effect came from LAI_s and SH. The F-test (lower values) indicated that the confounding factors are more influential at shorter than at longer wavelengths.

R^2 and F-test evaluation results of the VIs are presented in Table V. In most cases, the R^2 and the calculated F-test values of indices are much higher than the single bands. Among the tested VIs, the modified normalized difference (mND) $(\mathrm{R}2274.71-\mathrm{R}1921.01)/(\mathrm{R}2274.71+\mathrm{R}1921.01-2*\mathrm{R}1519.34)$ and the modified simple ratio (mSR) $(\mathrm{R}2274.71-\mathrm{R}1921.01)/(\mathrm{R}1921.01-\mathrm{R}1519.34)$ indices are the two best suitable indices for both LDMC and SLA. However, like the single bands, the selected indices were also influenced by the

TABLE IV
R^2 AND ANOVA F-TEST VALUES CALCULATED FOR TESTING HYSPEX SINGLE WAVELENGTHS (BANDS) SENSITIVITY FOR LDMC AND SLA VARIATION AGAINST THE CONFOUNDING VARIABLES

Wavelength (nm)	R^2	LDMC	LDMC/LAI_s	LDMC/SD	LDMC/SH	LDMC/CD	LDMC/ALA
1393.44	0.538	0.3424^{ns}	131.548	5.368	46.875	0.674^{ns}	2.09^{ns}
1489.36	0.608	0.5926^{ns}	137.156	10.34	62.497	0.721^{ns}	2.897^{ns}
1519.34	0.557	0.371^{ns}	199.569	5.254	54.579	0.395^{ns}	2.005^{ns}
1921.01	0.522	1.108^{ns}	7.398	5.015	15.735	5.782^{ns}	1.195^{ns}
2262.72	0.676	2.217	76.246	81.387	72.645	2.024^{ns}	4.564^{ns}
2274.71	0.678	2.796	71.913	120.589	73.398	2.621^{ns}	4.687^{ns}
2280.71	0.685	2.935	70.36	142.354	73.98	3.008^{ns}	4.925^{ns}
2298.69	0.698	4.016	60.839	249.187	73.019	4.07^{ns}	4.631^{ns}
2382.63	0.659	8.073	35.159	56.569	57.371	17.176	5.294^{ns}
Wavelength (nm)	R^2	SLA	SLA/LAI_s	SLA/SD	SLA/SH	SLA/CD	SLA/ALA
1393.44	0.036	0.097^{ns}	64.055	2.186^{ns}	22.792	0.166^{ns}	1.005^{ns}
1489.36	0.053	0.238^{ns}	79.546	6.259	37.215	0.293^{ns}	1.389^{ns}
1519.34	0.076	0.297^{ns}	210.215	5.084	59.321	0.137^{ns}	1.291^{ns}
1921.01	0.005	0.057^{ns}	0.498^{ns}	0.312^{ns}	1.002^{ns}	0.369^{ns}	0.013^{ns}
2262.72	0.379	6.006	288.90	312.159	273.698	9.270^{ns}	19.004
2274.71	0.387	7.009	278.921	471.615	284.150	11.807^{ns}	20.356
2280.71	0.390	7.043	271.390	559.497	284.997	13.000^{ns}	19.918
2298.69	0.381	8.925	233.954	948.720	272.439	17.975	21.722
2382.63	0.204	7.061	75.659	116.277	121.914	36.976	11.995

ns—not Significant at $P = 0.01$. The degrees of freedom were 34(LDMC), 5(SLA), 12(LAI_s), 10(SD), 6(SH), 4(CD), and 4(ALA).
The R^2 column indicates the correlation between the two leaf traits and canopy spectra at the specified wavelength. The column headed LDMC provides the variations caused by LDMC against the total variance of the confounding variables tested, whereas columns LDMC/LAI_s, LDMC/SD, LDMC/SH, LDMC/CD, and LDMC/ALA show the calculated F-test values caused by LDMC variance against the variance caused by each factor, and the same goes for SLA.

TABLE V
R^2 AND ANOVA F-TEST VALUES CALCULATED FOR TESTING HYSPEX-DERIVED VEGETATION INDICES SENSITIVITY FOR LDMC AND SLA VARIATION AGAINST THE CONFOUNDING VARIABLES

Index	R^2	LDMC	LDMC/LAI_s	LDMC/SD	LDMC/SH	LDMC/CD	LDMC/ALA
D	0.730	1.052	1158.689	13.597	230.138	1.126^{ns}	8.657^{ns}
SR	0.675	0.519	86.010	3.382^{ns}	1409.469	0.492^{ns}	300.497
ND	0.719	1.086	61.679	6.364	292.000	1.398^{ns}	130.709
mND	0.869	3.792	514.301	24.001	24610.176	4.697	154.807
mSR	0.850	2.795	373.015	18.371	15753.252	3.394^{ns}	126.301
Nd2	0.788	1.107	145.036	8.521	3622.538	1.491^{ns}	155.092
Index	R^2	SLA	SLA/LAI_s	SLA/SD	SLA/SH	SLA/CD	SLA/ALA
D	0.648	6.343	7041.529	84.003	1402.279	7.831^{ns}	53.256
SR	0.657	3.398	564.958	23.053	9351.259	4.081^{ns}	1980.137
Nd	0.695	7.728	408.769	42.017	1944.00	10.006^{ns}	871.456
mND	0.837	25.438	3411.538	160.097	163701.879	31.095	1026.226
mSR	0.828	19.001	2480.356	123.179	104746.894	23.325	854.839
ND2	0.626	6.690	787.247	46.437	19623.513	7.007^{ns}	841.127

ns—not significant at $P = 0.01$. The degrees of freedom were 34(LDMC), 5(SLA), 12(LAI_s), 10(SD), 6(SH), 4(CD), and 4(ALA).
The R^2 column indicates the correlation between the two leaf traits and the specified indices. The column headed LDMC provides the variations caused by LDMC against the total variance of the confounding variables tested, whereas columns LDMC/LAI_s, LDMC/SD, LDMC/SH, LDMC/CD, and LDMC/ALA show the calculated F-test values caused by LDMC variance against the variance caused by each factor, and the same goes for SLA.

confounding variables. The influence of CD was even higher for LDMC than for SLA. In five of the six indices tested, the variation due to LDMC was not significant (at $P = 0.01$) over that of the variation due to CD. Along with CD, SD was the perturbing structural variable that weakens the relationship between the indices and the two leaf traits.

B. Relationships Between LDMC and SLA, With Single Bands and VIs

In the previous section, single bands and VIs that were highly sensitive to LDMC and SLA variation were presented. Fig. 2 presents the results from the structural variables effect on the relationship between the two leaf traits with the highly sensitive bands (2298.69 nm for LDMC and 2280.71 nm for SLA). The relationships were set up by varying one confounding variable at a time and fixing the others at an average value for the test site ($\mathrm{LAIs} = 5.5$; $\mathrm{SD} = 800\,\mathrm{trees/ha}$; and $\mathrm{SH} = 23\,\mathrm{m}$, $\mathrm{CD} = 5.4\,\mathrm{m}$, and $\mathrm{ALA} = 500$). The high R^2 values of Fig. 2(a), (c), and (e) reveal that the relationship between LDMC and reflectance at 2298.69 nm is little affected by variations in LAIs, SH, and ALA compared to SD and CD. An increase in SH values decreases the reflectance linearly. Lower LAIs (<3) and lower SH ($<18\,\mathrm{m}$) values have greater impact than higher

LAIs (>4) and SH (>23 m) on the inverse linear relationship between reflectance and LDMC. The LSD post hoc comparison ($p = 0.01$) revealed that $\text{LAIs} \geq 6.5$ and $\text{SH} \geq 30$ have no significant impact on the relationship of LDMC and reflectance at 2298.69 nm.

Similarly, it can be observed that LAIs, SH, and ALA variations have less effect on the relationship between SLA and reflectance at 2280.71 nm [Fig. 2(f), (h), and (i)]. $\text{LAIs} \geq 6$ and $\text{SH} \geq 30$ did not show significant impact on the relationship between SLA and reflectance at 2280.71 nm for the LSD test ($p = 0.01$). It is evident that the greatest influence on both relationships arises from SD and CD [Fig. 2(b), (e), (g), and (i)].

At lower SD (<400 trees/ha) and CD (≤ 3) values, almost all variations in reflectance originate from the confounding factors, and the bands were almost insensitive to variations in LDMC and SLA. In addition, the impact of SD, CD, and ALA increases with decreasing LDMC concentration, and vice versa for SLA. In contrast, the impact of SH followed a uniform pattern for all values of the two leaf traits.

Compared to single bands, the structural variables effect on the relationships between LDMC and SLA with the mND index was greatly condensed (see Fig. 3). The influence of LAIs, SH, and ALA variations is minimal [Fig. 3(a), (c), (e), (f), (h), and (j)]. The LSD test ($p = 0.01$) showed that $\text{LAIs} \geq 5$ and $\text{SH} \geq 13$ m have no significant effect on the relationship between LDMC and SLA and the mND index. However, for SD and CD, the slope of the relationships rapidly declined when the SD and CD values dropped below 400 trees/ha and 3 m, respectively [Fig. 3(b), (d), (g), and (i)].

C. Implications for the Detectability of LDMC and SLA From Remotely Sensed Data

The slope of the relationships between the leaf traits and mND index was used as a measure of detectability to examine how varying two confounding variables at a time affects the accuracy of LDMC and SLA retrieval. The results obtained were linked to the actual stand properties of the Bavarian National Park Forest to study for which forest stands (broadleaf, conifer, or mixed) the detectability of the two leaf traits was most affected by the different combinations of the structural variables.

The detectability of LDMC by using the mND index and structural information derived from the broadleaf, conifer, and mixed stands of the test site is illustrated in Fig. 4. As can be observed from the figure, the greater the slope, the higher is the detectability of the two leaf traits. In terms of LAI_s and SH, all three stand types have nearly optimal conditions for retrieving canopy LDMC and SLA. They all have LAI_s above 3.5 and SH above 13 m [Fig. 4(b)]. The ranges of the structural information of broadleaf (purple), conifer (light green), and mixed (blue) stands of the Bavarian National Park Forest were plotted in the form of boxes. The light green boxes in Fig. 4(a)–(c) demonstrated that the conifer structural information is better for the leaf traits estimation than the other stands. By contrast, the purple and blue boxes in Fig. 4(a) and (c) revealed that the broadleaf and mixed stands (particularly some of the broadleaf stands) have very low SD values, which could significantly weaken the relationship between the traits and spectral variation at canopy scale.

IV. Discussion and Conclusion

Variations in forest canopy structures play an important role in retrieving biochemical and biophysical variables from canopy reflectance, yet the relative importance of each structural variable on the retrieval of LDMC and SLA from canopy reflectance has not been adequately addressed. The sensitivity of canopy reflectance in the NIR and SWIR spectral range to the variation in the two leaf traits and canopy structural variables were explored in this paper using a local sensitivity method with the simulated dataset from the INFORM model. Comparison of simulated reflectance at leaf and canopy scale indicated that the spectral variation at canopy level is lower than that at leaf level, due to the structural variables effect. The canopy reflectance reacts differently in the NIR and SWIR region for structural variables variation. From Fig. 1, it can be inferred that structural variables suppress canopy reflectance across the NIR and SWIR spectral region, but still there is a significant spectral variation that could be used to estimate the leaf traits.

Our R^2 and F-test results showed the presence of significantly strong correlations between the variation in the two leaf traits and canopy reflectance (Tables IV and V). The F-test result also indicated the greater suitability of longer wavelengths compared to shorter wavelengths for assessing both LDMC and SLA at canopy scale. Specifically, the contribution of the two leaf traits on the variability of forest canopy reflectance in the SWIR region of the spectrum is immense. In many cases, R^2 and the calculated F-statistics value is much higher in VIs (Table V) than in single bands (Table IV), which confirms that VIs outperform single bands in correlating leaf traits to canopy reflectance. This is because more spectral information is involved (especially from different regions of the spectrum) when using VIs than when using information from a single band. This result is in agreement with Verrelst *et al.* [51] and Malenovský *et al.* [52], who studied the effect of woody elements on forest chlorophyll content retrieval. Several non-significant F-test values were observed when the sensitivity of the canopy reflectance was tested for the variation in the two leaf traits against the structural variables. Predominantly, SD and CD variations influenced the relation between LDMC to both single bands and VIs. Large F-test calculated values were observed in the SWIR, which point out both LDMC and SLA being more detectable in the SWIR of the spectrum than in the NIR investigated in this study (data not shown). Asner *et al.* [23], le Maire *et al.* [70], and many others also reported the suitability of the SWIR region for the retrieval of biochemical and biophysical variables such as leaf mass per area and water content.

The five structural variables (LAI_s, SD, SH, CD, and ALA) examined in this study perturbed canopy reflectance at all single bands tested, but the greatest influence was observed for SD and CD, followed by ALA (Fig. 2). Unlike SH, the influence of LAI_s, SD, CD, and ALA varies with LDMC and SLA concentrations. This may be due to the confounding variables interaction with the two leaf traits. The F-test analysis on

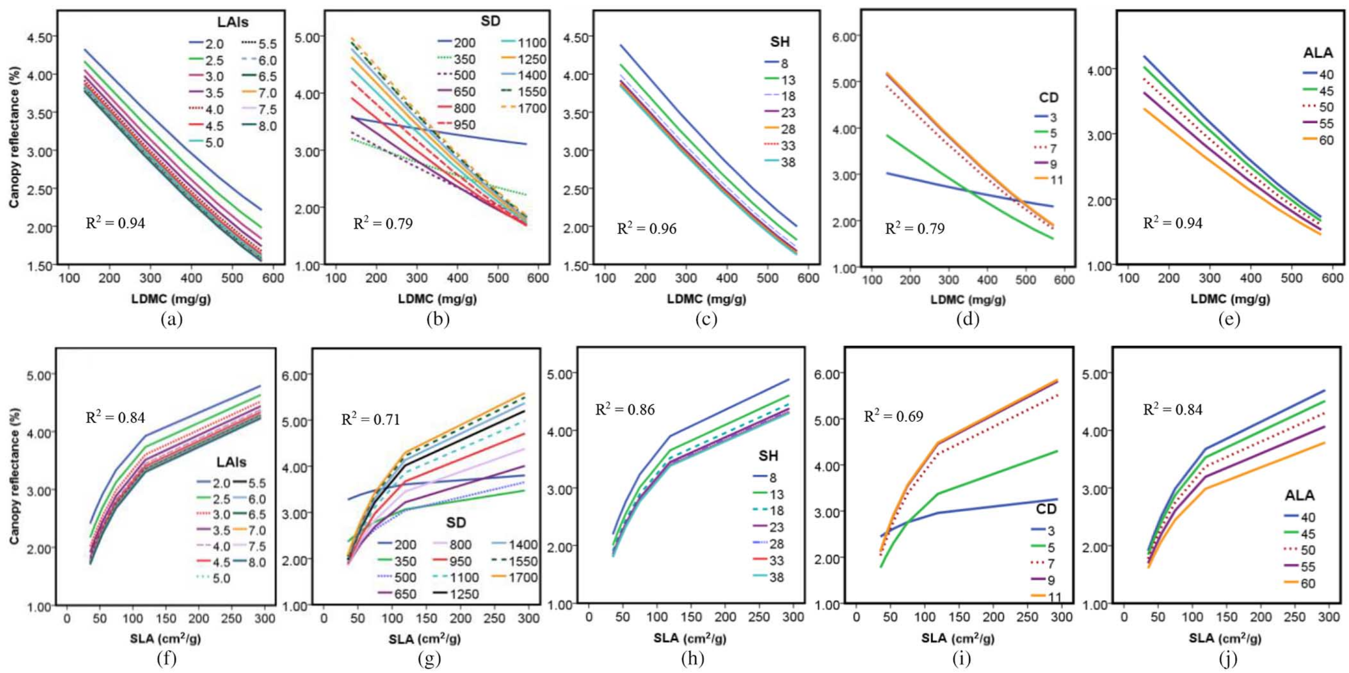

Fig. 2. Relationship between LDMC and the 2298.69-nm band, and SLA and the 2280.71-nm band, for a range of: (a) and (f) LAI_s; (b) and (g) SD; (c) and (h) SH; (d) and (i) CD; and (e) and (j) ALA with fixed values set to $\mathrm{LAI}_s = 5.5$, $\mathrm{SD} = 800\,\mathrm{trees/ha}$, $\mathrm{SH} = 23\,\mathrm{m}$, $\mathrm{CD} = 5.4\,\mathrm{m}$, $\mathrm{ALA} = 50°$, $\theta_s = 32°$, and $\Psi = 153$.

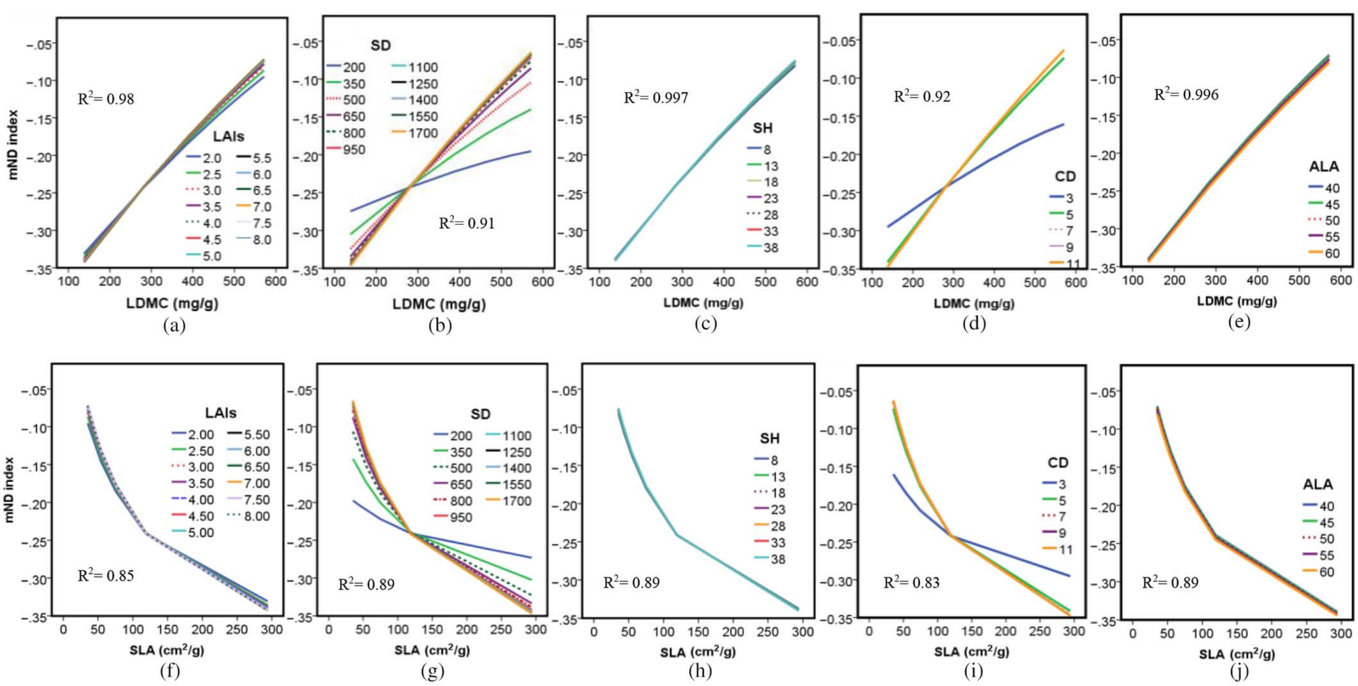

Fig. 3. Relationship between LDMC, SLA, and the mND index for a range of: (a) and (f) LAI_s; (b) and (g) SD; (c) and (h) SH; (d) and (i) CD; and (e) and (j) ALA with fixed values set to $\mathrm{LAI}_s = 5.5$, $\mathrm{SD} = 800\,\mathrm{trees/ha}$, $\mathrm{SH} = 23\,\mathrm{m}$, $\mathrm{CD} = 5.4\,\mathrm{m}$, $\mathrm{ALA} = 50°$, $\theta_s = 32°$, and $\Psi = 153$.

the interaction effects of the five confounding factors against LDMC and SLA concentration variation showed significant differences for the interaction of LAIs, SD, CD, and ALA with the two traits at $\alpha = 0.01$. Comparison of results from single bands (Fig. 2) and VIs (Fig. 3) gives an insight into how VIs yield robust estimations of leaf traits, irrespective of the structural variables influence. The mND VI was able to avoid much of the influence of all the five structural variables, except in a few cases of low SD and CD conditions. This indicates that the influence of the five structural variables on the two leaf traits' retrieval using remotely sensed data can be greatly minimized by spectral derivatives such as using VIs. The post hoc test confirmed that higher values of LAIs (≥ 5) and SH ($\geq 13\,\mathrm{m}$) have no impact and can be ignored in parameterizing RTM.

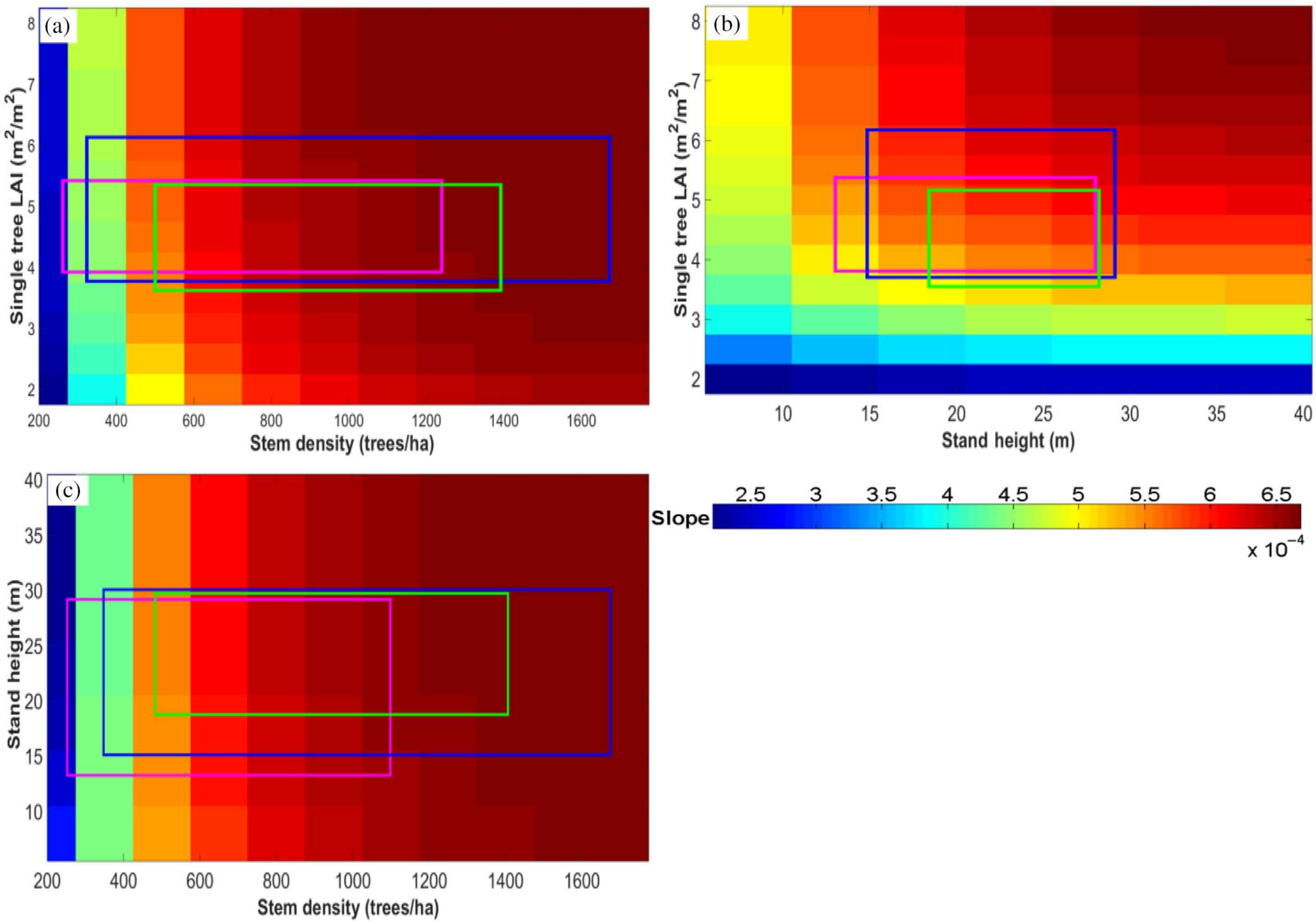

Fig. 4. Average slopes derived from the relationship between mND index and LDMC for three specific combinations of the structural variables. (a) LAI_s and SD; (b) LAI_s and SH; and (c) SH and SD with fixed variables set at average test site values. The three boxes in each subfigure show the structural information range of broadleaf (purple), conifer (light green), and mixed (blue) stands of the Bavarian National Park Forest.

Nevertheless, the correlation between the two leaf traits and canopy reflectance (single bands or mND index) may decline or vanish as long as the forest is sparsely populated ($\mathrm{SD} < 400\,\mathrm{trees/ha}$) with medium or small tree CD. Fig. 2(b), (c), (g), and (i) noticeably demonstrate that the correlation might be weakened in sparsely populated forest stands. This suggests that high estimation accuracy of the two leaf traits is to be expected for vegetation with high SD ($>400\,\mathrm{trees/ha}$) or CC. This finding confirms the result of a study [71], which suggested that for reliable retrieval of vegetation variables, the CC should be at least 30%.

An early study by Asner *et al.* [40] and Asner [47] revealed that in addition to the tremendous influence of CC, LAI is a major driver of canopy reflectance. A sensitivity analysis by Xiao *et al.* [53] also showed that the sensitivity of canopy reflectance to variation in equivalent water thickness (C_w) and leaf mass per area (C_m) is obscured mainly by LAI in the NIR and SWIR region. Our study supports these findings, but also demonstrates that if single bands are used instead of VIs (Fig. 2), SH, CD, and ALA could also perturb the relationship between the variation in the two leaf traits and canopy reflectance. Therefore, for accurate estimation of LDMC and SLA, it is important to use spectral derivatives such as VIs or adopt various inversion strategies other than sensitive single wavelengths.

As depicted in Fig. 4, except for a few extremely low values of the structural variables, the slope between LDMC and the mND index is greater than 5×10^{-4}, and even greater slope values ($>2 \times 10^{-3}$) were observed for the relationship between SLA and mND (not shown here). This reaffirms the detectability of the two leaf traits when using mND index. From the three stand structural combination templates, we may conclude that the most important structural factors determining the detectability of the two leaf traits are SD and CD.

In a nutshell, our results have demonstrated: 1) the presence of a strong relationship between the two leaf traits' variation and canopy reflectance; 2) the existence of significant canopy reflectance disturbance from SD, LAI_s SH, CD, and ALA; 3) the capability of VIs to correct confounding effects of canopy structural heterogeneity originating from these structural variables; and 4) the promising detectability of the LDMC and SLA of the test site from hyperspectral data. However, it is worth mentioning that, in our analysis, we investigated the influence of only five structural variables (SD, LAI_s SH, CD, and ALA). The background was represented by an average value for all elements in the understory. Other input parameters except solar zenith and azimuth angle were set at average values. These choices, along with our choice of wavelengths, Vis, and the INFORM model for simulation, might have biased our results. For instance, in low SD stands, the background reflectance may contribute to the variation in the reflectance related to the two leaf traits if the understory is green vegetation. It can also act as an additional confounding factor if the forest floor is litter, bare soil, and/or lying wood [51]. The INFORM model simulates top of canopy reflectance based on certain input parameters by assuming that the forest canopy is fully occupied by green leaves. The simulated result could be biased if there is a significant amount of woody material or litter in the canopy. In this study, only specific spectral bands from the HYSpex available spectral regions were investigated. However, utilizing other spectral bands may provide useful information to distinguish subtle spectral variations due to LDMC and SLA. Therefore, further research is required to understand how structural variables (other than LAI_s, SD, SH, CD, and ALA), the presence of nonphotosynthetic materials in the canopy, background composition, and illumination and viewing positions affect the relationship between the leaf traits (LDMC and SLA) and canopy reflectance in the NIR–SWIR region. The present study investigated the retrieval of the two leaf traits based on the spectral features and the indices developed for leaf mass per area, but additional study is recommended to discover spectral features and VIs that are specifically sensitive to LDMC and SLA, so that these can be accurately mapped using remotely sensed data.

ACKNOWLEDGMENT

HYSpex data were provided by German Aerospace Center (DLR). The authors acknowledge the assistance of Dr. U. Heiden and Dr. N. Pinnel from DLR for organizing the HYSpex overflight and preprocessing the acquired images, Dr. H. Latifi from the Institute of Geography and Geology, University of Wurzburg in facilitating the field campaign. They would like to thank the Bavarian Forest National Park staff for approving access to the test site and providing field and camping facilities. They would also like to thank M. Schlerf for making the INFORM code available. A language professional proofread the text.

REFERENCES

[1] D. Vile, B. Shipley, and E. Garnier, "Ecosystem productivity can be predicted from potential relative growth rate and species abundance," *Ecol. Lett.*, vol. 9, pp. 1061–1067, Sep. 2006.
[2] P. J. Wilson, K. E. N. Thompson, and J. G. Hodgson, "Specific leaf area and leaf dry matter content as alternative predictors of plant strategies," *New Phytol.*, vol. 143, pp. 155–162, 1999.
[3] J. H. C. Cornelissen *et al.*, "A handbook of protocols for standardised and easy measurement of plant functional traits worldwide," *Aust. J. Bot.*, vol. 51, pp. 335–380, 2003.
[4] L. L. Pierce, S. W. Running, and J. Walker, "Regional-scale relationships of leaf-area index to specific leaf-area and leaf nitrogen-content," *Ecol. Appl.*, vol. 4, pp. 313–321, May 1994.
[5] Y. L. Feng, G. L. Fu, and Y. L. Zheng, "Specific leaf area relates to the differences in leaf construction cost, photosynthesis, nitrogen allocation, and use efficiencies between invasive and noninvasive alien congeners," *Planta*, vol. 228, pp. 383–390, Aug. 2008.
[6] L. Benomar, A. DesRochers, and G. R. Larocque, "Changes in specific leaf area and photosynthetic nitrogen-use efficiency associated with physiological acclimation of two hybrid poplar clones to intraclonal competition," *Can. J. For. Res.*, vol. 41, pp. 1465–1476, Jul. 2011.
[7] I. J. Wright *et al.*, "The worldwide leaf economics spectrum," *Nature*, vol. 428, pp. 821–827, Apr. 2004.
[8] J. L. D. Osnas, J. W. Lichstein, P. B. Reich, and S. W. Pacala, "Global leaf trait relationships: Mass, area, and the leaf economics spectrum," *Science*, vol. 340, pp. 741–744, May 2013.
[9] M. T. Dominguez, C. Aponte, I. M. Perez-Ramos, L. V. Garcia, R. Villar, and T. Maranon, "Relationships between leaf morphological traits, nutrient concentrations and isotopic signatures for Mediterranean woody plant species and communities," *Plant Soil*, vol. 357, pp. 407–424, Aug. 2012.
[10] D. Vile *et al.*, "Specific leaf area and dry matter content estimate thickness in laminar leaves," *Ann. Bot.*, vol. 96, pp. 1129–1136, Nov. 1, 2005.
[11] B. Shipley, "Trade-offs between net assimilation rate and specific leaf area in determining relative growth rate: Relationship with daily irradiance," *Funct. Ecol.*, vol. 16, pp. 682–689, Oct. 2002.
[12] R. A. Marenco, S. A. Antezana-Vera, and H. C. S. Nascimento, "Relationship between specific leaf area, leaf thickness, leaf water content and SPAD-502 readings in six Amazonian tree species," *Photosynthetica*, vol. 47, pp. 184–190, Jun. 2009.
[13] B. Shipley, "Net assimilation rate, specific leaf area and leaf mass ratio: Which is most closely correlated with relative growth rate? A meta-analysis," *Funct. Ecol.*, vol. 20, pp. 565–574, Aug. 2006.
[14] J. G. Hodgson *et al.*, "Is leaf dry matter content a better predictor of soil fertility than specific leaf area?" *Ann. Bot.*, vol. 108, pp. 1337–1345, Nov. 2011.
[15] S. Lavorel *et al.*, "Using plant functional traits to understand the landscape distribution of multiple ecosystem services," *J. Ecol.*, vol. 99, pp. 135–147, 2011.
[16] M. A. Mouchet, S. Villéger, N. W. H. Mason, and D. Mouillot, "Functional diversity measures: An overview of their redundancy and their ability to discriminate community assembly rules," *Funct. Ecol.*, vol. 24, pp. 867–876, 2010.
[17] C. H. Albert *et al.*, "Intraspecific functional variability: Extent, structure and sources of variation," *J. Ecol.*, vol. 98, pp. 604–613, May 2010.
[18] M. Duru, R. A. H. Khaled, C. Ducourtieux, J. P. Theau, F. L. F. de Quadros, and P. Cruz, "Do plant functional types based on leaf dry matter content allow characterizing native grass species and grasslands for herbage growth pattern?" *Plant Ecol.*, vol. 201, pp. 421–433, Apr. 2009.
[19] S. Lavorel *et al.*, "Assessing functional diversity in the field—Methodology matters!" *Funct. Ecol.*, vol. 22, pp. 134–147, 2008.
[20] D. Tilman, "Functional diversity," in *Encyclopedia of Biodiversity*, vol. 3, S. A. Levin, Ed. New York, NY, USA: Academic press, 2001, pp. 109–120.
[21] A. Skidmore, *Environmental Modelling with GIs and Remote Sensing*, 1st ed. New York, NY, USA: Taylor & Francis, 2002.
[22] R. Houborg, H. Soegaard, and E. Boegh, "Combining vegetation index and model inversion methods for the extraction of key vegetation biophysical parameters using Terra and Aqua MODIS reflectance data," *Remote Sens. Environ.*, vol. 106, pp. 39–58, Jan. 2007.
[23] G. P. Asner *et al.*, "Taxonomy and remote sensing of leaf mass per area (LMA) in humid tropical forests," *Ecol. Appl.*, vol. 21, pp. 85–98, Jan. 2011.
[24] G. P. Asner *et al.*, "Spectroscopy of canopy chemicals in humid tropical forests," *Remote Sens. Environ.*, vol. 115, pp. 3587–3598, 2011.
[25] T. U. Kampe, G. P. Asner, R. O. Green, M. Eastwood, B. R. Johnson, and M. Kuester, "Advances in airborne remote sensing of ecosystem processes and properties—Toward high-quality measurement on a global scale," *Remote Sens. Model. Ecosyst. Sustain. VII*, vol. 7809, pp. 78090J-1–78090J-13, 2010.
[26] R. F. Kokaly, G. P. Asner, S. V. Ollinger, M. E. Martin, and C. A. Wessman, "Characterizing canopy biochemistry from imaging spectroscopy and its application to ecosystem studies," *Remote Sens. Environ.*, vol. 113, pp. S78–S91, 2009.
[27] J.-B. Féret and G. P. Asner, "Mapping tropical forest canopy diversity using high-fidelity imaging spectroscopy," *Ecol. Appl.*, vol. 24, pp. 1289–1296, 2014.
[28] M. Schlerf and C. Atzberger, "Inversion of a forest reflectance model to estimate structural canopy variables from hyperspectral remote sensing data," *Remote Sens. Environ.*, vol. 100, pp. 281–294, Feb. 2006.
[29] S. Jacquemoud and F. Baret, "Prospect—A model of leaf optical-properties spectra," *Remote Sens. Environ.*, vol. 34, pp. 75–91, Nov. 1990.
[30] B. J. Yoder and R. H. Waring, "The normalized difference vegetation index of small Douglas-fir canopies with varying chlorophyll concentrations," *Remote Sens. Environ.*, vol. 49, pp. 81–91, Jul. 1994.

[31] C. J. Tucker, "A critical-review of remote-sensing and other methods for nondestructive estimation of standing crop biomass," *Grass Forage Sci.*, vol. 35, pp. 177–182, 1980.

[32] R. Darvishzadeh, A. Skidmore, M. Schlerf, and C. Atzberger, "Inversion of a radiative transfer model for estimating vegetation LAI and chlorophyll in a heterogeneous grassland," *Remote Sens. Environ.*, vol. 112, pp. 2592–2604, May 2008.

[33] M. C. Wang, X. F. Niu, S. B. Chen, P. J. Guo, Q. Yang, and Z. J. Wang, "Inversion of chlorophyll contents by use of hyperspectral CHRIS data based on radiative transfer model," in *Proc. 35th Int. Symp. Remote Sens. Environ. (ISRSE35)*, 2014, vol. 17, pp. 1–6.

[34] R. Darvishzadeh, A. A. Matkan, and A. D. Ahangar, "Inversion of a radiative transfer model for estimation of rice canopy chlorophyll content using a lookup-table approach," *IEEE J. Sel. Topics Appl. Earth Observ. Remote Sens.*, vol. 5, pp. 1222–1230, Aug. 2012.

[35] R. Darvishzadeh, C. Atzberger, A. Skidmore, and M. Schlerf, "Mapping grassland leaf area index with airborne hyperspectral imagery: A comparison study of statistical approaches and inversion of radiative transfer models," *ISPRS J. Photogramm. Remote Sens.*, vol. 66, pp. 894–906, 2011.

[36] S. L. Ustin *et al.*, "Retrieval of foliar information about plant pigment systems from high resolution spectroscopy," *Remote Sens. Environ.*, vol. 113, pp. S67–S77, Sep. 2009.

[37] D. A. Roberts *et al.*, "Spectral and structural measures of northwest forest vegetation at leaf to landscape scales," *Ecosystems*, vol. 7, pp. 545–562, Aug. 2004.

[38] S. V. Ollinger, "Sources of variability in canopy reflectance and the convergent properties of plants," *New Phytol.*, vol. 189, pp. 375–394, 2011.

[39] A. Wolf, J. A. Berry, and G. P. Asner, "Allometric constraints on sources of variability in multi-angle reflectance measurements," *Remote Sens. Environ.*, vol. 114, pp. 1205–1219, Jun. 2010.

[40] G. P. Asner, C. A. Wessman, D. S. Schimel, and S. Archer, "Variability in leaf and litter optical properties: Implications for BRDF model inversions using AVHRR, MODIS, and MISR," *Remote Sens. Environ.*, vol. 63, pp. 243–257, 1998.

[41] R. D. Morris, A. Kottas, M. Taddy, R. Furfaro, and B. D. Ganapol, "A statistical framework for the sensitivity analysis of radiative transfer models," *IEEE Trans. Geosci. Remote Sens.*, vol. 46, no. 12, pp. 4062–4074, Dec. 2008.

[42] R. Darvishzadeh, A. Skidmore, C. Atzberger, and S. van Wieren, "Estimation of vegetation LAI from hyperspectral reflectance data: Effects of soil type and plant architecture," *Int. J. Appl. Earth Observ. Geoinf.*, vol. 10, pp. 358–373, Sep. 2008.

[43] H. Bach and W. Verhoef, "Sensitivity studies on the effect of surface soil moisture on canopy reflectance using the radiative transfer model GeoSAIL," in *Proc. IEEE Int. Geosci. Remote Sens. Symp. (IGARSS'03)*, 2003, vols. I–VII, pp. 1679–1681.

[44] R. Riou and F. Seyler, "The effect of soil on rain-forest canopy nir reflectance on spot oblique imagery," *C. R. Acad. Sci. Ser. II*, vol. 320, pp. 1079–1086, Jun. 1995.

[45] Y. K. Ross, A. A. Golinis, T. A. Nilson, and K. Y. Ross, "Effect of liming on soil reflectance," *Sov. J. Remote Sens.*, vol. 6, pp. 1003–1011, 1990.

[46] N. N. Vygodskaya and I. I. Gorshkova, "Analysis of canopy-soil optical reflectance behavior using Goudriaans model. 2. Effect of illumination conditions on reflectance," *Sov. J. Remote Sens.*, vol. 4, pp. 991–1004, 1986.

[47] G. P. Asner, "Biophysical and biochemical sources of variability in canopy reflectance," *Remote Sens. Environ.*, vol. 64, pp. 234–253, Jun. 1998.

[48] C. V. M. Barton and P. R. J. North, "Remote sensing of canopy light use efficiency using the photochemical reflectance index: Model and sensitivity analysis," *Remote Sens. Environ.*, vol. 78, pp. 264–273, Dec. 2001.

[49] P. Bowyer, F. M. Danson, and N. M. Trodd, "Methods of sensitivity analysis in remote sensing: Implications for canopy reflectance model inversion," in *Proc. IEEE Int. Geosci. Remote Sens. Symp. (IGARSS'03)*, 2003, vols. I–VII, pp. 3839–3841.

[50] A. Bannari, K. Staenz, D. Haboudane, and K. S. Khurshid, "Sensitivity analysis of chlorophyll indices to soil optical properties using ground-reflectance data," in *Proc. IEEE Int. Geosci. Remote Sens. Symp.*, 2006, vols. 1–8, pp. 120–123.

[51] J. Verrelst, M. E. Schaepman, Z. Malenovský, and J. G. P. W. Clevers, "Effects of woody elements on simulated canopy reflectance: Implications for forest chlorophyll content retrieval," *Remote Sens. Environ.*, vol. 114, pp. 647–656, 2010.

[52] Z. Malenovský *et al.*, "Influence of woody elements of a Norway spruce canopy on nadir reflectance simulated by the DART model at very high spatial resolution," *Remote Sens. Environ.*, vol. 112, pp. 1–18, 2008.

[53] Y. F. Xiao, W. J. Zhao, D. M. Zhou, and H. L. Gong, "Sensitivity analysis of vegetation reflectance to biochemical and biophysical variables at leaf, canopy, and regional scales," *IEEE Trans. Geosci. Remote Sens.*, vol. 52, no. 7, pp. 4014–4024, Jul. 2014.

[54] A. M. Ali, R. Darvishzadeh, A. K. Skidmore, I. C. van Duren, U. Heiden, and M. Heurich, "Estimating leaf functional traits by inversion of PROSPECT: Assessing leaf dry matter content and specific leaf area in mixed mountainous forest," Ph.D. thesis, Nat. Resour. Univ. Twente, 2014, pp. 1–30.

[55] M. Heurich, B. Beudert, H. Rall, and Z. Krenova, "National parks as model regions for interdisciplinary long-term ecological research," in *Long-term Ecological Research Between Theory and Application*, F. Müller, C. Baessler, H. Schubert, and S. Klotz, Eds. New York, NY, USA: Springer, 2010, pp. 327–344.

[56] M. Heurich and M. Neufanger, *Die Wälder des Nationalparks Bayerischer Wald. Ergebnisse der Waldinventur 2002/2003 im geschichtlichen und waldökologischen Kontext*, Grafenau, Germany, 2005, p. 178 S.

[57] J.-M. N. Walter. (2009, Nov. 3). *CIMES-FISHEYE. Hemispherical Photography of Forest Canopies. A Package of Programs for the Assessment of Canopy Geometry and Solar Radiation Regimes Through Hemispherical Photographs* [Online]. Available: http://equinoxe.u-strasbg.fr/cimes

[58] J. L. Widlowski *et al.*, "The fourth radiation transfer model intercomparison (RAMI-IV): Proficiency testing of canopy reflectance models with ISO-13528," *J. Geophys. Res. Atmos.*, vol. 118, pp. 6869–6890, Jul. 2013.

[59] W. Verhoef, "Light-scattering by leaf layers with application to canopy reflectance modeling—The Sail model," *Remote Sens. Environ.*, vol. 16, pp. 125–141, 1984.

[60] W. Fan, J. M. Chen, W. Ju, and G. Zhu, "GOST: A geometric-optical model for sloping terrains," *IEEE Trans. Geosci. Remote Sens.*, vol. 52, no. 9, pp. 5469–5482, Mar. 2014.

[61] J. P. Gastellu-Etchegorry, E. Martin, and F. Gascon, "DART: A 3D model for simulating satellite images and studying surface radiation budget," *Int. J. Remote Sens.*, vol. 25, pp. 73–96, Jan. 2004.

[62] K. F. Huemmrich, "The GeoSail model: A simple addition to the SAIL model to describe discontinuous canopy reflectance," *Remote Sens. Environ.*, vol. 75, pp. 423–431, Mar. 2001.

[63] L. Xiaowen and A. H. Strahler, "Geometric-optical bidirectional reflectance modeling of the discrete crown vegetation canopy: Effect of crown shape and mutual shadowing," *IEEE Trans. Geosci. Remote Sens.*, vol. 30, no. 2, pp. 276–292, Mar. 1992.

[64] C. Atzberger, "Development of an invertible forest reflectance model: The INFOR-model," in *A Decade of Trans-European Remote Sensing Cooperation*, M. F. Buchroithner, Ed., Dresden, Germany: A.A. Balkema, Jun. 14–16, 2000, pp. 39–44.

[65] A. Rosema, W. Verhoef, H. Noorbergen, and J. J. Borgesius, "A new forest light interaction-model in support of forest monitoring," *Remote Sens. Environ.*, vol. 42, pp. 23–41, Oct. 1992.

[66] A. Romero, I. Aguado, and M. Yebra, "Estimation of dry matter content in leaves using normalized indexes and PROSPECT model inversion," *Int. J. Remote Sens.*, vol. 33, pp. 396–414, 2012.

[67] G. P. Asner, R. E. Martin, A. J. Ford, D. J. Metcalfe, and M. J. Liddell, "Leaf chemical and spectral diversity in Australian tropical forests," *Ecol. Appl.*, vol. 19, pp. 236–253, Jan. 2009.

[68] S. Jacquemoud, S. L. Ustin, J. Verdebout, G. Schmuck, G. Andreoli, and B. Hosgood, "Estimating leaf biochemistry using the PROSPECT leaf optical properties model," *Remote Sens. Environ.*, vol. 56, pp. 194–202, Jun. 1996.

[69] A. Baumgartner, P. Gege, C. Kohler, K. Lenhard, and T. Schwarzmaier, "Characterisation methods for the hyperspectral sensor HySpex at DLR's calibration home base," *Sens. Syst. Next Gen. Satell. XVI*, vol. 8533, pp. 85331H-1–85331H-8, 2012.

[70] G. le Maire *et al.*, "Calibration and validation of hyperspectral indices for the estimation of broadleaved forest leaf chlorophyll content, leaf mass per area, leaf area index and leaf canopy biomass," *Remote Sens. Environ.*, vol. 112, pp. 3846–3864, Oct. 2008.

[71] G. S. Okin, D. A. Roberts, B. Murray, and W. J. Okin, "Practical limits on hyperspectral vegetation discrimination in arid and semi-arid environments," *Remote Sens. Environ.*, vol. 77, pp. 212–225, Aug. 2001.

Abebe Mohammed Ali received the B.Sc. degree in forestry from Wondo Genet College of Forestry, Debub University, Awassa, Ethiopia, in 2002, and the M.Sc. degree in geo-information science from Wageningen University, Wageningen, The Netherlands, in 2006. He is currently pursuing the Ph.D. degree in geo-information science and earth observation (ITC) at the University of Twente, Enschede, The Netherlands.

He was previously GIS and Remote Sensing Officer from 2007 to 2009. He has been a Lecturer and Head of the Department of Geography and Environmental Studies, Wollo University, Dessie, Ethiopia, since 2009. His research interests include the development of optical remote-sensing approaches, assessing quantitatively the biophysical and biochemical variables of vegetation using radiative transfer models.

Roshanak Darvishzadeh received the Ph.D. degree in hyperspectral remote sensing of vegetation from Wageningen University, Wageningen, The Netherlands, in 2008.

She is currently an Assistant Professor with the Department of Natural Resources, University of Twente (Faculty ITC), Enschede, The Netherlands. She has ample experience on the use of laboratory and field instruments and quantitative methods in vegetation mapping and monitoring. Her research interests include mapping and modeling biochemical and biophysical properties of vegetation with the use of statistical and radiative transfer models and exploration of hyperspectral, multispectral, thermal hyperspectral, and LIDAR data.

Andrew K. Skidmore received the Ph.D. degree in remote sensing and GIS from the Australian National University, Canberra, Australia, in 1989.

He is the Professor of Spatial Environmental Resource Dynamics with the University of Twente and Chairman of the Department of Natural Resources, Faculty of ITC, Enschede, The Netherlands. He has authored more than 190 ISI journal articles and 17 book chapters. His research interests include hyperspectral remote sensing, habitat monitoring under fragmentation, and climate change, as well as image processing and more generally techniques for handling geo-information.

Iris Van Duren received the Ph.D. degree in wetland ecology from the University of Groningen, Haren, The Netherlands, in 1999.

She is currently an Assistant Professor with the Department of Natural Resources, University of Twente (Faculty ITC), Enschede, The Netherlands. Her research interests include improving the accuracy in mapping forest biomass and plant functional traits through development of new remote-sensing approaches and modeling techniques.